

SUPPLEMENTARY MATERIALS

Figs. S1 to S5

Figure S1

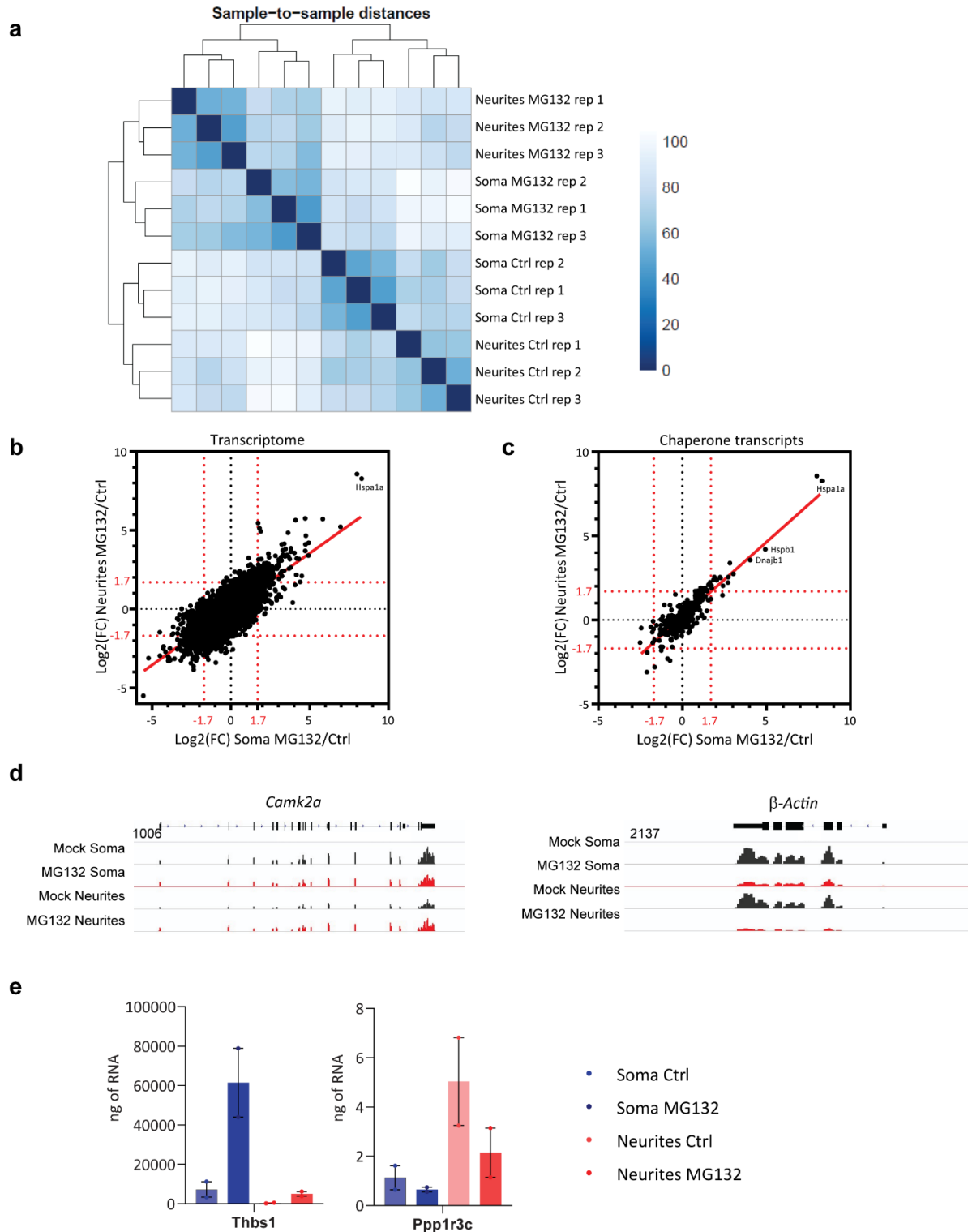
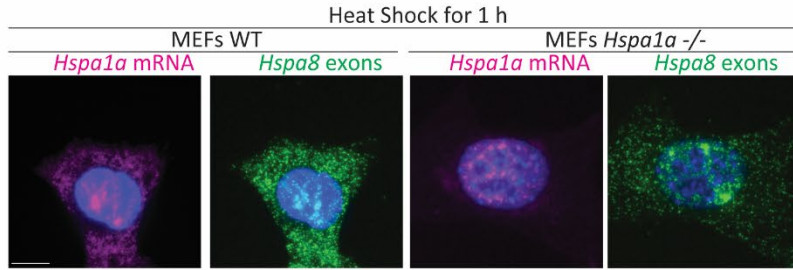


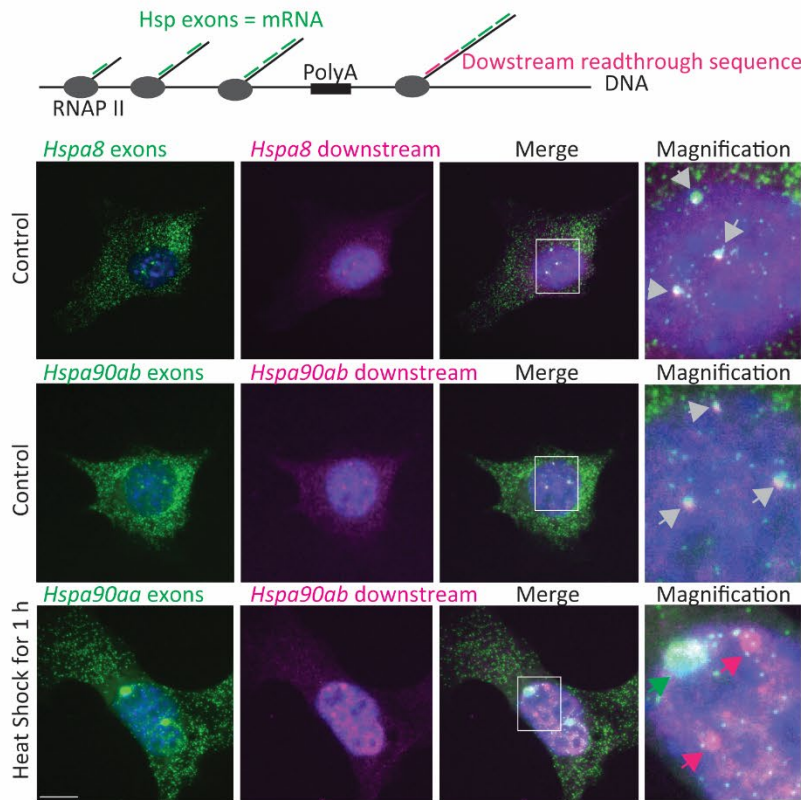
Figure S1. RNA-seq validation (a) Clustering of RNA-seq replicates. (b, c) Two-dimensional density plot showing the Log₂(FC) of the soma (x axis) and neurites (y axis) in MG132-treated (10 μM for 7 h) versus Ctrl neurons for all genes (B) and molecular chaperone-related genes (C). (d) RNA-seq distributions of the *Camk2a* and *β-actin* loci in the soma and neurites of control and MG132-exposed neurons. (e) Validation of RNA-seq data by RT-qPCR for the DEGs *Thbs1* (enriched in the soma upon MG132 treatment) and *Ppp1r3c* (enriched in the neurites under control conditions). Data are the mean ± the SEM of two independent experiments.

Figure S2

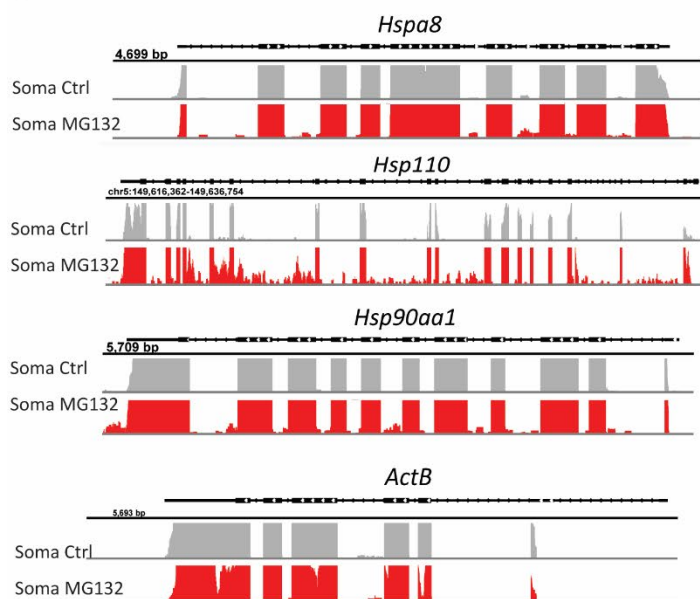
a



b



c



d

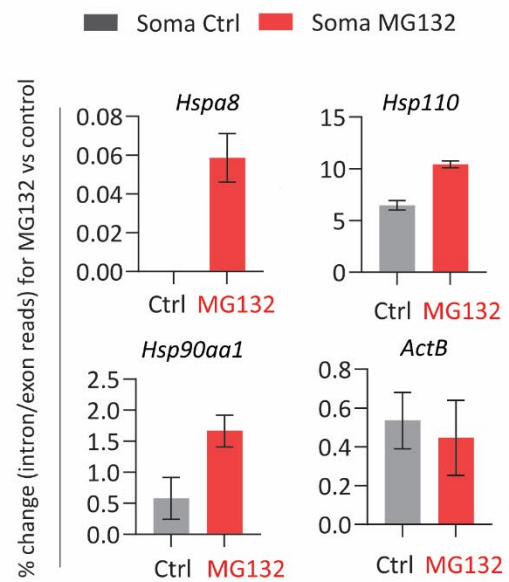
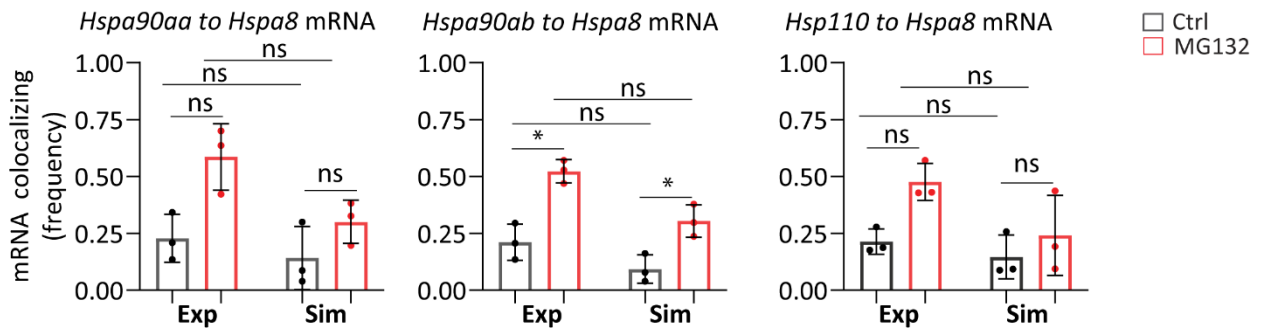


Figure S2. Validation of smFISH probes specificity and transcription site detection (a) SmFISH Detection of *Hspa1a* and *Hspa8* mRNAs in WT MEFs and MEFs^{Hspa1a^{-/-}} subjected to 1 h of heat-shock at 42°C to activate the transcription of *Hspa1a*. *Hspa1a* mRNA is only detected in the cytoplasm of WT MEFs. **(b)** Upper and middle panels. Identification of *Hspa8* and *Hsp90ab* transcription sites in MEFs using two-color smFISH to detect their exon sequences (green) and the genomic region downstream of the PolyA sequence (magenta). White squares indicate magnified images. Gray arrows in magnified regions point to transcription sites where both signals co-localize. Mature mRNAs are only detected with probes for exons. Note that transcription sites are brighter than single mRNAs indicating the presence of more than one transcript per transcription site. Lower panel. Identification of *Hsp90aa* exons (green) and *Hsp90ab* genomic region downstream of the polyA sequence (magenta) in MEFs subjected to 1 h of heat shock to induce *Hspa90aa* transcription. The magnified region shows a lack of co-localization between smFISH probes recognizing different nascent transcripts. Scale bar = 10 μ m. **(c)** Representative IGV snapshots of exonic and intronic reads were obtained from the RNA sequencing of somatic RNAs of Ctrl and MG132-stressed neurons (Fig. 1). **(d)** Change in the percentage of intronic to exonic read ratio in Ctrl vs MG132-stress neuron for genes in (c). Data are the mean \pm SEM of three independent experiments.

Figure S3

a



b

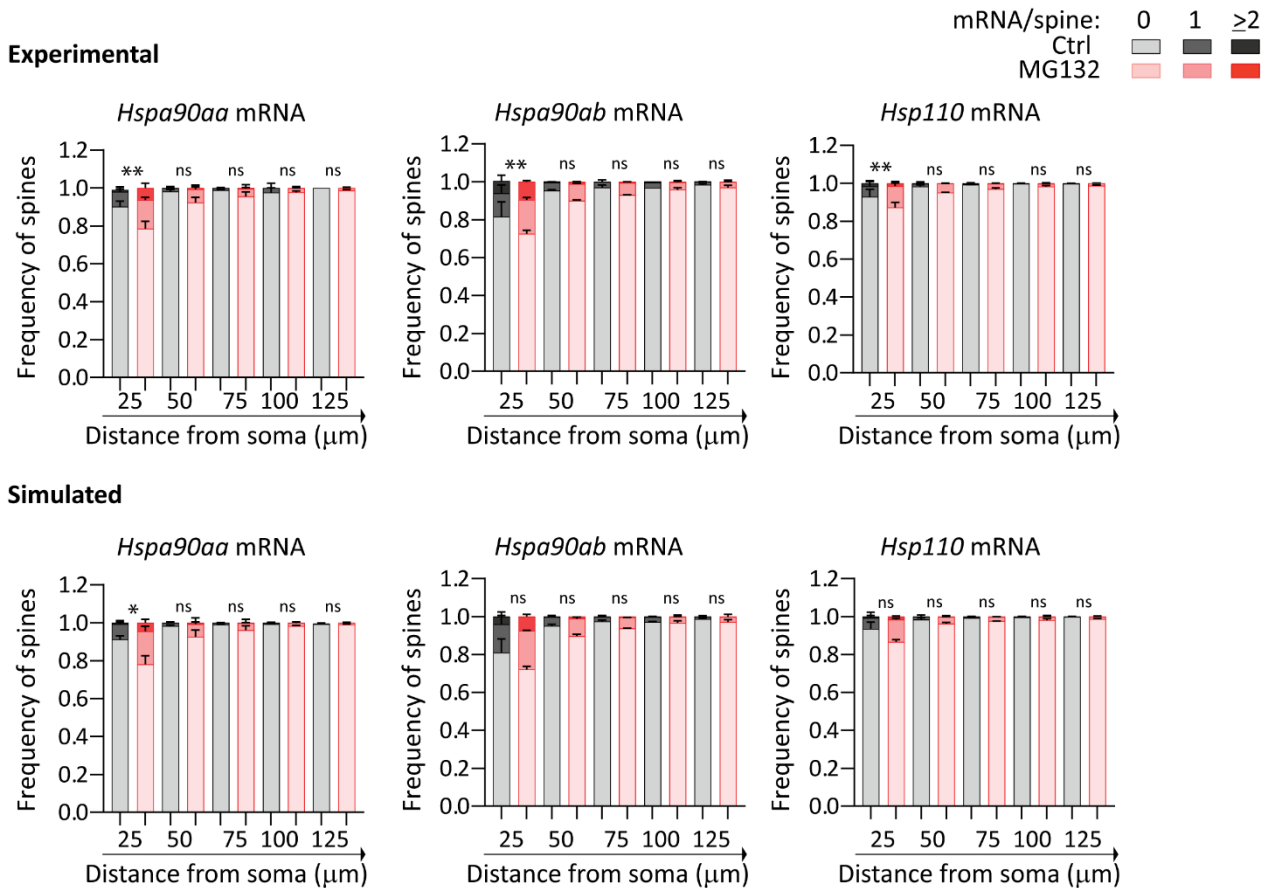


Figure S3. Distribution of HSP mRNAs in the dendritic shaft (a) Frequency of colocalization between *Hspa90aa*, *Hspa90ab*, or *Hsp110* mRNAs and *Hspa8* mRNA per dendrite in Ctrl and MG132-stressed primary hippocampal neurons shown in Fig. 3f and 3g. Exp indicates experimental data. Sim indicates simulated data that is the average of 100 random simulations of the positions of each detected *Hspa8* mRNA in a specific dendrite. Data from Fig. 3h. $P < 0.01$; *, $P < 0.05$; ns, no significant (by Wilcoxon t -test). **(b)** Frequency of dendrites with 0, 1, and 2 or more *Hspa90aa*, *Hspa90ab*, or *Hsp110* mRNAs localizing within 600 nm of the center of the PSD95 fluorescent signal in the Ctrl and MG132-stressed primary hippocampal neurons shown in Fig. 3h and 3i. Simulated data are the mean of 100 random simulations of the position of each *Hspa90aa*, *Hspa90ab*, or *Hsp110* mRNAs detected in a specific dendritic bin.

Figure S4

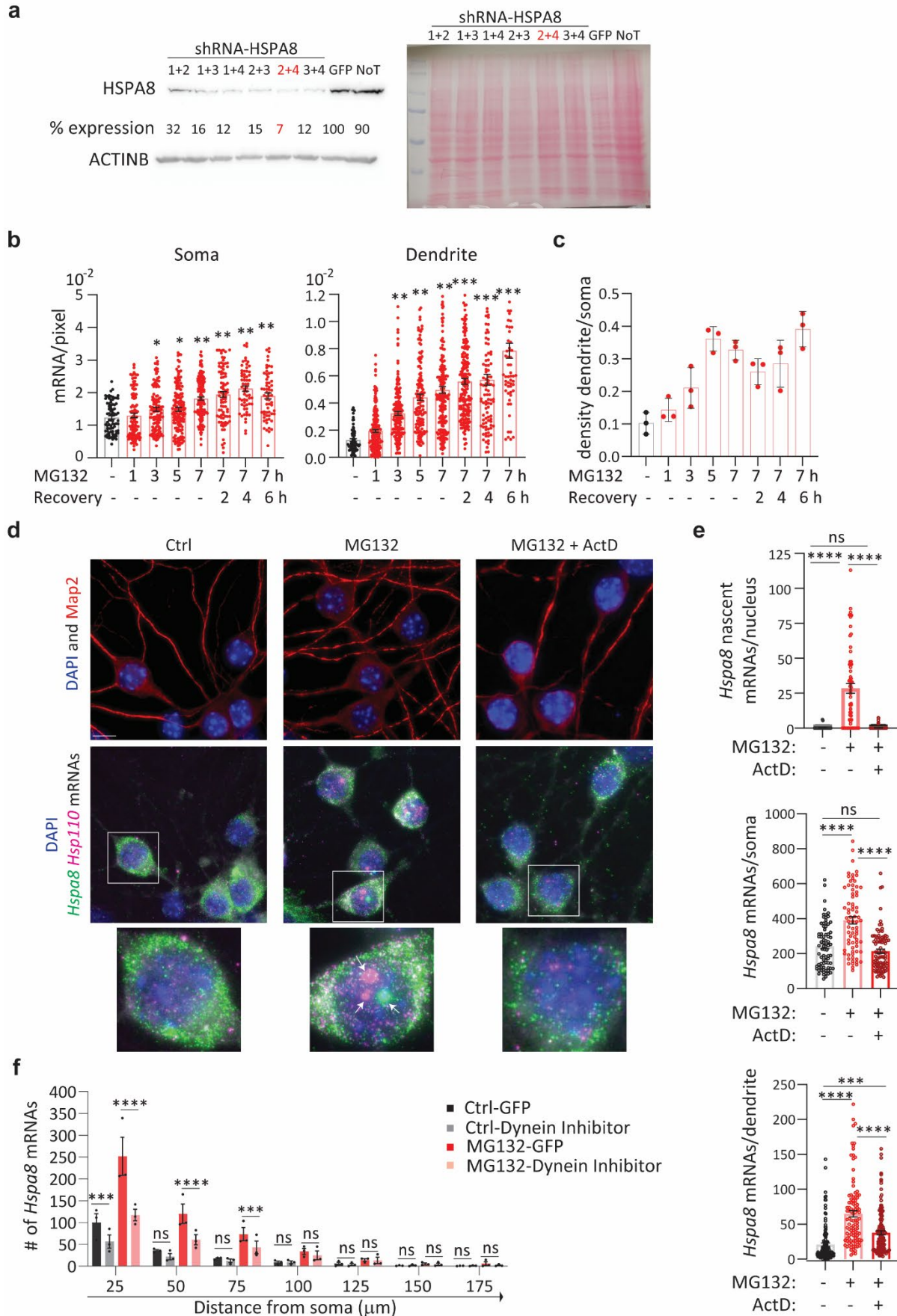
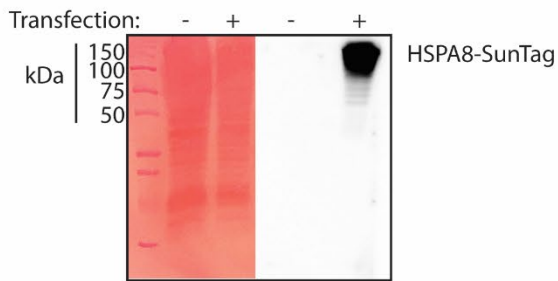


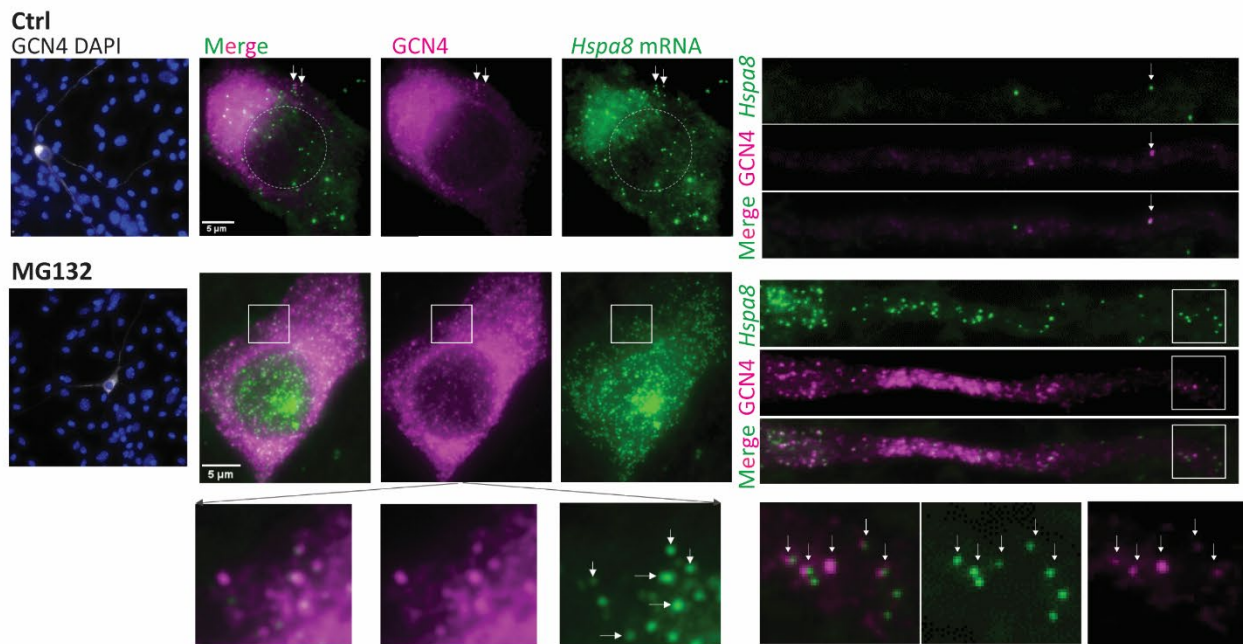
Figure S4. Characterization of the regulated localization of *Hspa8* mRNA in hippocampal neuron dendrites (a) Immunoblot of HSPA8 and β -ACTIN expression in MEFs after 4 days of transfection with the indicated combinations of HSPA8 shRNA plasmids, GFP, and non-transfected (NT). The blot on the right is the ponceau staining of total protein. (b) Quantification of the density of *Hspa8* mRNAs per pixel area in the soma or dendrites of Ctrl and MG132-stressed neurons (10 μ M) for the indicated times and during recovery from MG132 (Recov) for the indicated times. Data are the mean \pm SD of three independent experiments ($n = 60$ -155 neurons and $n = 63$ -207 dendrites; dots indicate individual soma and dendrite values). (c) The ratio of *Hspa8* mRNA per pixel of soma or dendrite area in the Ctrl and MG132-stressed hippocampal neurons analyzed in C. ***, $P < 0.001$; **, $P < 0.01$; *, $P < 0.05$; ns, no significant (by Welch's t -test). (d) The upper panels show the detection of the nucleus and dendrites and the lower panel shows two-color smFISH detection of *Hspa8* and *Hsp110* mRNAs of Ctrl, MG132 stressed (10 μ M for 7 h), and transcription inhibited (Actinomycin D (ActD) 2.5 μ g/mL) MG132 stressed (10 μ M for 7 h) primary hippocampal neurons. The square shows a magnified view of a neuron nucleus and arrows point to transcription sites. Scale bar = 10 μ m. (e) Quantification of nascent, somatic, and dendritic *Hspa8* mRNAs in Ctrl, MG132-stressed motor neurons transcriptionally active or not after incubation with ActD. Data are the mean \pm SEM of three independent experiments ($n = 107$ -134 dendrites; dots indicate individual soma and dendrite values). ****, $P < 0.0001$; ***, $P < 0.001$; ns, no significant (by 1 way ANOVA) (f) Quantification of *Hspa8* mRNAs per 25- μ m bin in experiment 4F and 4G ($n = 154$ -160 dendrites; dots indicate individual dendrite values). ****, $P < 0.0001$; ***, $P < 0.001$; ns, no significant (by t -test).

Figure S5

a



b



c

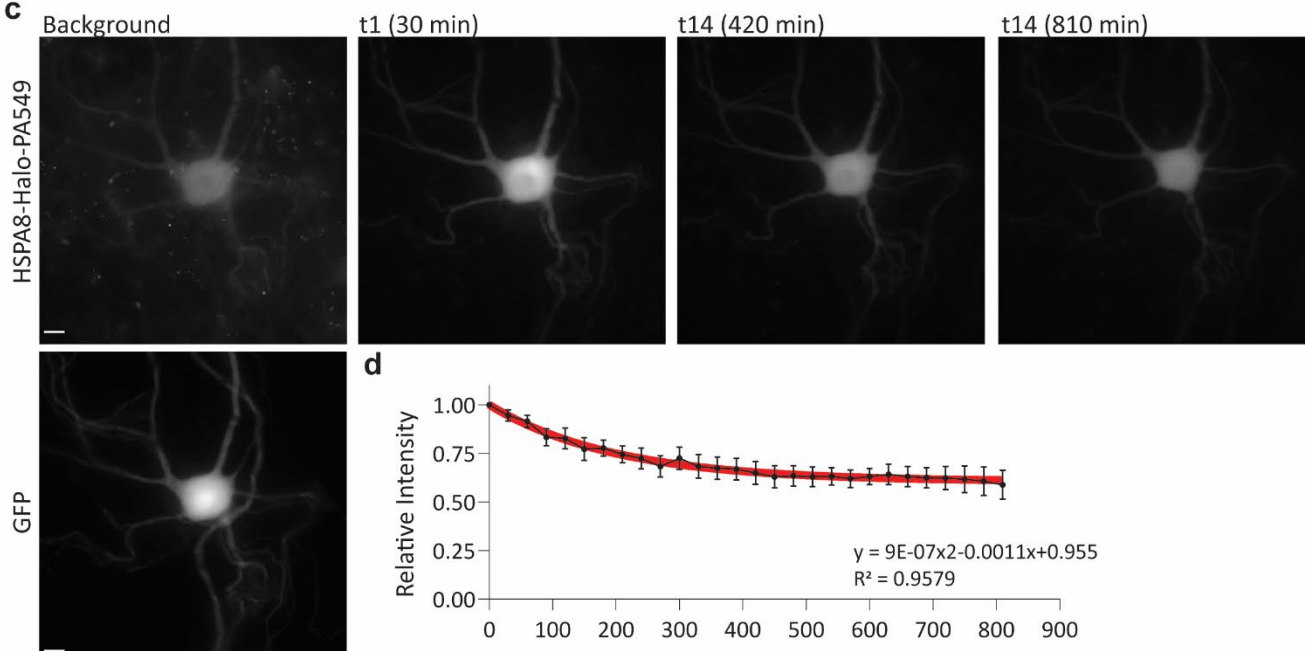


Figure S5. A translation reporter to study localized HSPA8 synthesis in neurons (a) Western blot detection of the HSPA8 single-molecule translational reporter. Left, Ponceau staining of the full protein lysate; right, western blot detecting the reporter's GCN4 epitopes. **(b)** Representative IF-smFISH images of somas and dendrites of Ctrl and MG132-stressed primary spinal cord motor neurons expressing the *Hspa8* single-molecule translational reporter. White arrows indicate translating mRNAs. Squares depict the magnified regions. Scale bar = 5 μm . **(c)** Representative snapshots of timelapse imaging of primary spinal cord motor neurons co-expressing GFP and HSPA8-Halo. The background is after incubation with PA-JF549 and before photostimulation and t1, t14, and t28 indicate the time imaging acquisition after 10 ms of photostimulation with a 405 nm laser. Scale bar = 10 μm . **(d)** Quantification of PA-JF549 average intensity over time-lapse imaging. The black line and dots are the mean \pm SEM of data from 8 spinal cord motor neurons and the red line is the second-order polynomial fit. Equation and R-squared values are displayed.

Figure S6

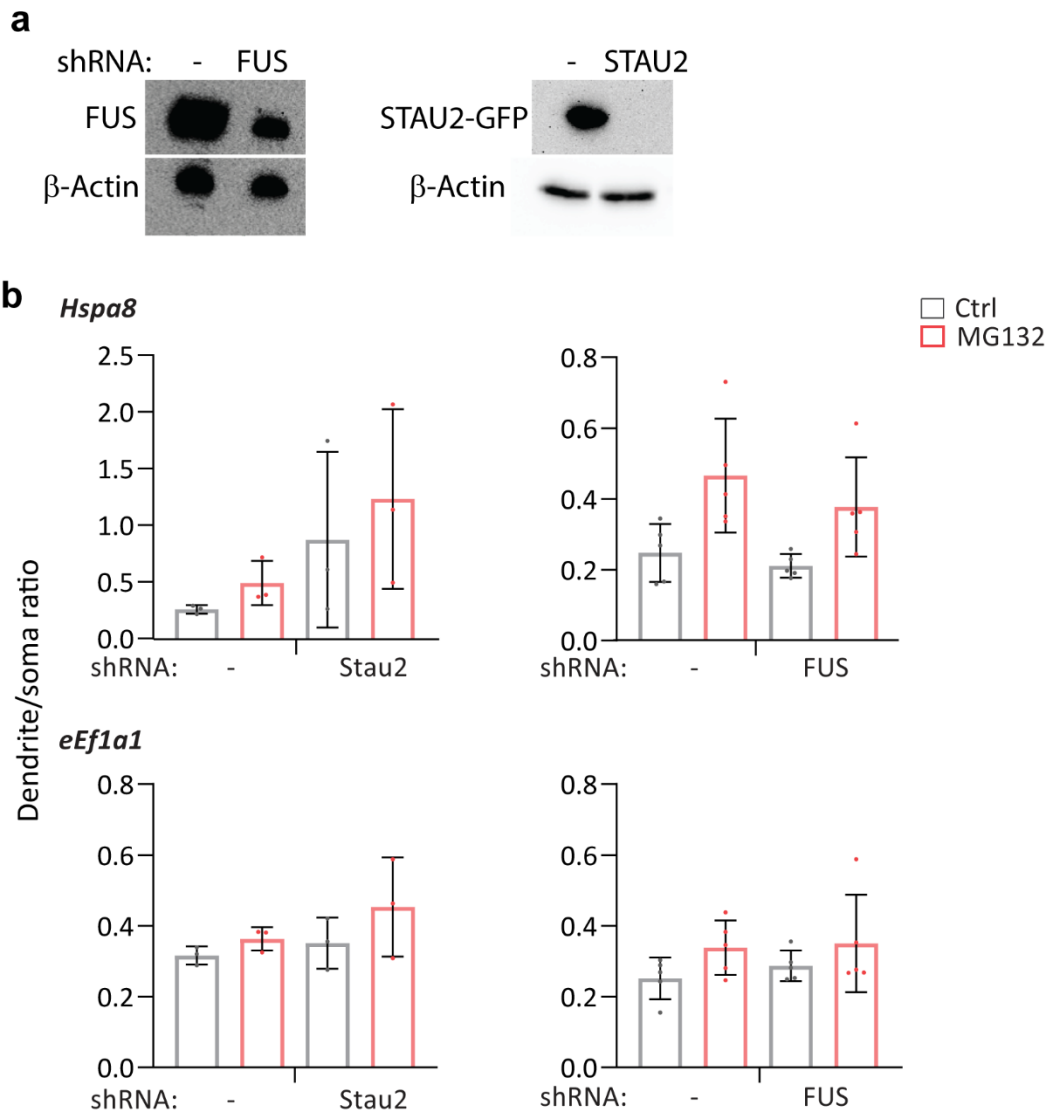


Figure S6. FUS and STAU2 knockdown and HNRNPA2B1 mutation impact the subcellular distribution of *HSPA8* mRNA (a) Western blot detection of FUS and STAU2 in Ctrl and shRNA-transfected 293T cells. β -actin was used as a loading control. **(b)** Ratio of *Hspa8* mRNA per pixel of soma or dendrite area in the Ctrl and MG132-stressed motor neurons analyzed in Fig. 6e–h.